

Conf-820704--19

LA-UR-82-1948

**MASTER**

Los Alamos National Laboratory is operated by the University of California for the United States Department of Energy under contract W-7405-ENG-36

LA-UR--82-1948

DE82 019556

TITLE: A CALCULATIONAL ADVANCE IN THE MODELING OF FUEL-COOLANT INTERACTIONS

AUTHOR(S): W. R. Boh1

SUBMITTED TO: Conference International Sur La Surete Des Reactueres Rapides  
A Metal Liquide Et Ses Aspects Conception Et Fontionnement  
July 19-23, 1982, LYON, ECUILLY FRANCE

**DISCLAIMER**

This report was prepared as an account of work sponsored by an agency of the United States Government. It is the property of the United States Government and is loaned to your organization; it and its contents are not to be distributed outside your organization. The Government assumes no responsibility for the accuracy or completeness of any information reported hereon, or for the use of any information hereon. The Government makes no warranty, expressed or implied, with respect to the use of the information hereon. The Government will not be held liable for any damages resulting from the use of the information hereon. The views and opinions of the authors are those of the authors and are not necessarily those of the United States Government or any agency thereof. This report is approved for public release and its distribution is unlimited.

DISTRIBUTION OF THIS DOCUMENT IS UNLIMITED  
*JRP*

By acceptance of this article, the publisher recognizes that the U S Government retains a nonexclusive royalty-free license to publish or reproduce the published form of this contribution, or to allow others to do so, for U S Government purposes

The Los Alamos National Laboratory requests that the publisher identify this article as work performed under the auspices of the U S Department of Energy

**Los Alamos** Los Alamos National Laboratory  
Los Alamos, New Mexico 87545

CLEARANCE NOTICE

This certifies that the paper,  
A CALCULATIONAL ADVANCE IN THE MODELING OF FUEL-COOLANT INTERACTIONS

(Title)

by W. R. Bohl

(Authors)

of Los Alamos National Laboratory

(Organization)

Mail Stop K556  
P.O. Box 1663  
Los Alamos, NM 87545

(Address)

as submitted to  
for inclusion in the proceedings of the International Topical Meeting  
on Liquid Metal Fast Breeder Reactor Safety and Related Design and  
Operational Aspects, July 19-23, 1982, is cleared for publication.  
The paper contains no information of national security interest,  
patent considerations, or other proprietary information interests  
that need be withheld from publication.

(Signature)

(Title)

## A CALCULATIONAL ADVANCE IN THE MODELING OF FUEL-COOLANT INTERACTIONS

W. R. Boul  
Energy Division  
Los Alamos National Laboratory  
Los Alamos, New Mexico 87545, U.S.A.

### ABSTRACT

A new technique is applied to numerically simulate a fuel-coolant interaction. The technique is based on the ability to calculate separate space- and time-dependent velocities for each of the participating components. In the limiting case of a vapor explosion, this framework allows calculation of the pre-mixing phase of film boiling and interpenetration of the working fluid by hot liquid, which is required for extrapolating from experiments to a reactor hypothetical accident. Qualitative results are compared favorably to published experimental data where an iron-alumina mixture was poured into water. Differing results are predicted with LMFBR materials.

### INTRODUCTION

The subject of molten-fuel-coolant interactions (MFCI) has been of interest in liquid-metal-fast-breeder-reactor (LMFBR) hypothetical-core-disruptive-accident (HCDA) analysis for some time. The consequences of MFCI could be serious in terms of both direct damage to the primary system and potential rapid fuel compaction and recriticality. Previous analytical work<sup>1</sup> has generally assumed postulated configurations and concentrated on the fragmentation and mixing processes involved in MFCI. Present whole-core accident computer modeling<sup>2,3</sup> uses at most two interacting velocity fields and consequently cannot readily treat the interpenetration of fuel and liquid coolant relative to the vapor produced. If uncertainties are to be reduced in accident calculations involving potential MFCI, the formalism employed should be capable of addressing where fuel-coolant contact can occur and simulating the appropriate physics of MFCI. Current understanding of this physics suggests the requirement of separate velocity fields for fuel, liquid coolant, and vapor. This paper presents the initial formulation of an appropriate multifield algorithm for use in whole-core accident codes such as SIMMER.<sup>3</sup> There is a discussion of comparisons to thermite-water thermal detonation experiments performed at Sandia National Laboratories (SNL)<sup>4,5</sup>, and extrapolation to LMFBR materials is considered.

### CALCULATIONAL TECHNIQUES

The calculational approach is to solve directly the conservation equations for compressible, multiphase fluid flow. An Eulerian finite-difference format similar to that in SIMMER is employed; that is, an iteration is used to solve the coupled continuity and momentum equations,

whereas the convective terms in the energy equations are evaluated outside the iteration. However, several differences exist between this method and the SIMMER method. First, the iterative procedure for the pressure is required to converge for both the individual component densities and the actual non-linear equation of state (EOS). Changes in cell material composition and in two-phase to single-phase cell characteristics are now accommodated consistently within the iteration. Second, the velocity derivatives and velocity changes used to converge the pressure iteration are obtained numerically, rather than analytically, from the coupled momentum equations at each cell interface. Analytical procedures are rather cumbersome with three or more velocity fields. Third, convection in the energy equations has been implemented consistently using end-of-time step velocities, resolving energy conservation problems. Fourth, a step-donor procedure suggested by Steinke<sup>6</sup> has been implemented to reduce smearing of density and energy gradients.

Momentum, mass, and energy exchange are calculated similarly to SIMMER by ignoring intercell convection while performing intracell transfers. The most complicated of these intracell exchange processes is vaporization-condensation. Here a non-equilibrium situation must be simulated to achieve interfacial vaporization when bulk coolant temperatures are below saturation conditions. This is accomplished by calculating mass-transfer rates based on the imbalance of heat flow to the coolant boundary layer. For consistency, all intracell energy-transfer processes are evaluated implicitly within a single set of coupled equations, which are solved iteratively in terms of five independent variables. These variables are the gas (vapor) temperature, the fuel temperature, the liquid coolant temperature, the vaporization-condensation rates, and the saturation temperature corresponding to the partial pressure of coolant vapor. Knowledge of these changes then allows update of dependent cell variables consisting of the material internal energies, the cell vapor volume fraction, the temperature-dependent liquid coolant density, the total cell pressure, and other EOS parameters. This implicit approach allows a consistent treatment of those computational cells where the mass and thermal inertia of a given component is limited.

As in any multiphase numerical formulation, several special situations require treatment. Four items are of most importance for this formalism. First, the momentum-field coupling terms can involve velocity differences raised to the fourth power. A mixing of the current and previous time-step velocities is used to avoid oscillations. Second, when extremely small amounts of a liquid component are present, its velocity field is tightly coupled to the vapor field to avoid velocity divergence due to the explicit evaluation of momentum convection. Third, if an entire spatial region is at the two-phase to single-phase transition, cell-to-cell oscillations are terminated by forcing single-phase conditions on the affected cells. Fourth, a special version of the energy equations is used when all remaining liquid coolant in one computational cell can vaporize in a time step.

This numerical approach is relatively stable and efficient, accommodates large multidimensional distortions, and appears compatible with existing HCDA codes. The Eulerian format does lead to problems with respect to smearing and with determining constitutive relationships from instantaneous values of cell variables. These deficiencies are most important if detonation and propagation of a shock wave is to be calculated for a large-scale vapor explosion. We must assume that a rather approximate treatment of the detailed physics will display the dominant features of the situation.

## CONSTITUTIVE RELATIONSHIPS

The solution of a MFCI problem involves more than the solution to the conservation equations. Relationships are required for energy and momentum exchange. The main purpose of this paper is to demonstrate the promise of this multifield formulation by simulating SNL vapor explosion tests.<sup>4,5</sup> Consequently, these experiments are used as a basis for constitutive relationships.

The experimental vapor explosions are produced in the free contact mode, i.e., pouring molten fuel (thermite) into the coolant (water). The experimental sequence typically involves three steps. First, relatively quiescent coarse mixing of the constituents is observed. Second, a triggering event occurs followed by fine fragmentation and propagation leading to efficient thermite-to-water heat transfer. Third, the high pressure reaction products expand with the potential for doing mechanical work on the surroundings.

The coarse mixing phase is characterized by film boiling. For the current analysis, the main heat-transfer path for energy transport is assumed to be thermal radiation from thermite spheres to the vapor-water interface. The emissivity view-factor product is input as is the thermite sphere radius. The area for energy transport is based on the thermite sphere radius, unless insufficient liquid water remains. For small amounts of water, the water is presumed to exist in drops, with the drop size determined by the ratio of the water-to-thermite surface tensions. Because radiation heat transport is presumed to be slow, temperature gradients within thermite spheres are ignored. Three secondary modes of energy transfer are also included. First, convection from the thermite to surrounding vapor is calculated based on the relative thermite-vapor velocity. Second, because the shape of the water-vapor interface is unknown, heat transfer from vapor to the liquid-water boundary layer is based on conduction with the conduction length determined by one-fifth the thermite radius. Third, conduction is also assumed for heat transfer from the water surface into the bulk water. The area for conduction to and from the water surface is assumed to be given by the minimum obtained from one of two configurations. The more general case is given by a configuration where the water is the continuous medium with the thermite plus vapor volume simulated by spheres of the thermite radius. The second configuration is similar to the radiation area limitation when only small amounts of water are present. Here, vapor is the continuous medium with relative surface tensions assumed to provide the water-to-thermite radius ratio.

The triggering event is speculated to be water entrapment and/or homogeneous nucleation.<sup>5</sup> Currently, this must be postulated in the calculation. The phenomenology of the fine fragmentation and mixing stage is uncertain. A fragmentation model based on relative liquid-liquid velocities might be possible, particularly considering liquid-liquid fragmentation data taken by Theofanous.<sup>7</sup> However, Corradini<sup>8</sup> suggests that hydrodynamic fragmentation by fuel-coolant relative velocities alone occurs too slowly to explain the rapid fragmentation observed in single drop SNL tests. In any case, such modeling is beyond the scope of this paper. Here, triggering is assumed when the melt hits a solid surface. A zero-order propagation model is then applied initiating fragmentation in any cell which (a) has a vapor fraction of less than 5%, and (b) is adjacent to a cell which is located closer to the triggering site and in which fragmentation has previously been

initiated. The basis for this representation is a propagation model by Corrad'ni<sup>8</sup> where fragmentation is induced by a vapor film collapse.

Following initiation of fragmentation in a cell, separate time constants are used to fragment the fuel and water down to a minimum size. The use of separate time constants allows delayed coolant fragmentation and the representation of a controlled amount of surface vaporization with limited heating of bulk coolant. Such non-equilibrium effects are apparently present, at least with water.<sup>9</sup> The same heat-transfer paths are retained as in film boiling, with the addition of a SIMMER-type liquid-liquid heat-transfer path attributed to postulated liquid-liquid contact upon film boiling collapse. Of course, now the coolant area decreases exponentially, based on the coolant fragmentation time constant, rather than on surface tension considerations.

In this treatment, the expansion phase is considered to be merely an extension of the propagation phase with no required changes in the energy transport algorithm.

The functional form for momentum transfer is the same for each step of the experimental sequence. The flow regime under consideration is presumed to change from single phase, to bubbly, to churn-turbulent, and finally to dispersed flow with increasing vapor volume fraction. Water is presumed to be the continuous medium except in dispersed flow. The overall magnitude of liquid-to-vapor momentum coupling is set by correlation to experimental slip velocities from the available bubble-column and boiling-pool data base. The thermite is presumed to couple to the vapor via a SIMMER-type formalism in dispersed flow. A droplet formula coupling the thermite and water is assumed to provide the liquid-liquid coupling in the other flow regimes. This treatment is not completely consistent with the energy transfer although improvements should be possible as more definitive pictures can be drawn of the processes involved.

#### COMPARISON TO SNL EXPERIMENTS

Two experimental series were examined. The Buxton tests<sup>4</sup> involved pouring up to 27 kg of iron-alumina thermite into a steel tank, which contained a water volume of approximately 0.7 m<sup>3</sup>. Tests by Mitchell<sup>5</sup> dropped up to 5 kg of thermite from a greater height into a smaller volume of water, about .22 m<sup>3</sup>, contained in a transparent box.

These problems were set up on variable dimension 12-by-28 meshes. The water was represented by 20 axial nodes, whereas 8 nodes were used to represent the thermite, which was initially falling through inert gas. The system pressure was 0.1 MPa. The initial water temperature was 300 K. The Mitchell simulation was given a mesh spacing in the water of 0.0282 m radially and 0.0305 m axially. The Buxton simulation used a uniform water mesh spacing of 0.045 m. The four separate components modeled were water, steam, thermite, and the inert gas. No chemical reactions were modeled between the water and the thermite.

An initial problem encountered in simulating these experiments was apparent excessive heat transfer. When the thermite was prefragmented to a 15-mm diameter, as suggested by Mitchell as representative in the film boiling step, it was difficult to mix the thermite with water. Water vaporization was so rapid as to disperse the thermite. This result could be related to conclusions reached by Henry<sup>10</sup> in LWR core meltdown situations.

Henry derived a formula for the minimum melt radius that allows water to alleviate the imposed steam flux. If we assumed an emissivity of unity and a 10-kg melt mass, which entered the water over a  $0.0254\text{-m}^2$  area (corresponding to the two radial nodes in the Buxton simulation), Henry's formula gave a melt radius of 0.27 m. The actual entering thermite cross-sectional area was uncertain; however, the thermite breakup probably would need to be modeled to simulate how the water surface area would become available. In these calculations, assuming prefragmentation of the thermite, an emissivity-view-factor product of 0.03 was used. This gave a 8-mm radius from Henry's formula, and avoids excessive early thermite dispersal in the numerical simulation.

The momentum-transfer relationships produced more readily useable results. In the Buxton tests, explosions were reported between 1 and 3 s after the pour started; and the calculation indicate thermite contacting the tank bottom 1 s after initial thermite-to-water contact. In the simulation of Mitchell test MD-19, with 5.1 kg of thermite, an explosion was reported at 0.2 s. A comparison of the calculated thermite distribution at 0.2 s to the reported data is shown in Fig. 1. Although the thermite distribution initially entering the water was uncertain, a qualitatively appropriate parabolic characteristic was calculated.

The MD-19 simulation was used to fit the fragmentation time constants. Optimal values were 0.1 ms for fuel fragmentation and 0.2 ms for water breakup. The time of 0.1 ms would be about the time it would take the reported fragmentation wave (at 200 to 600 m/s) to cross one node (30-50 mm). Some degree of non-equilibrium was obviously present in the fine fragmentation stage. The reported maximum pressure at the lower pressure transducer was about 17.5 MPa. The present time constants led to a calculated maximum pressure of 15.7 MPa. If the water breakup time was reduced to 0.1 ms, the increased water surface area quenched the maximum pressure to 5.0 MPa. The single-phase propagation criterion was generally unsatisfactory. Initially, steam produced by surface vaporization tended to increase the vapor volume fraction and to limit direct upward propagation. Later, water moving inward allowed satisfaction of the low void fraction criterion resulting in an unreported secondary pressure pulse. Because of the initially limited extent of propagation, the minimum fuel fragmentation radius was set to 25  $\mu\text{m}$ . It can be noted that this was a size consistent with the more fragmented experimental debris, and the experiments showed an unknown quantity of unreacted luminous molten material in the expansion phase.

These same parameters were applied in the Buxton test simulation. Plots of the water volume fraction qualitatively showing the sequence progression with time are given in Fig. 2. A comparison of the tank wall pressure trace with two Buxton tests is shown in Fig. 3. With the stochastic nature of these tests, the comparison is reasonable, although long-term water quenching was delayed in the calculation because of the propagation algorithm.

#### EXTRAPOLATION TO LMFBR MATERIALS

The one requirement to produce a vapor explosion with the current free-contacting-mode model is a stable period of film boiling. In the uranium dioxide-sodium system, film boiling is apparently possible<sup>11</sup> although the available MFCI data base suggests stability is not readily achieved. One system where such film boiling is believed more probable is the uranium carbide (UC)-sodium (Na) system. In this study, Mitchell-type

and Buxton-type tests were calculated with a UC-Na system, assuming sodium at 920 K.

The general tendency of the results was to produce significantly less coolant vaporization. More heating of the liquid sodium occurred because of the large increase in sodium thermal diffusivity relative to water. In both cases the carbide dispersed less in film boiling. In the Mitchell-type simulation the extra liquid tamping and rapid liquid-sodium heating led to a 93 MPa single-phase pressure pulse of 0.25 ms duration following detonation. The liquid sodium expansion was not accommodated in the available vapor volume, and the single-phase propagation algorithm requirements were satisfied. This result must be accepted as logical, given the model employed. It should be noted that a pressure pulse of this magnitude (actually 190 MPa) has been produced in a small-scale UC-Na system.<sup>12</sup>

### CONCLUSIONS

A calculational technique consistent with whole-core analysis codes has been developed to treat the MFCI problem. The technique uses separate velocities for the coolant, fuel, and vapor, solving the compressible fluid dynamics equations in a two-dimensional format. Reasonable numerical stability and efficiency using this technique have been achieved. With the insertion of limited constitutive relationships, results using the technique have been successfully compared to thermite-water experiments on a qualitative basis. The need for increased modeling of globule breakup is evident. Constitutive relationships would be particularly useful both for how a coarse mixture forms and for how fine fragmentation proceeds. Extrapolation to LMFBR materials is a non-trivial problem. Qualitatively differing results are possible; and understanding the meaning of the results probably requires analysis of experiments with more typical environments. Further development of the numerical technique itself should allow better simulation of MFCI phenomena.

### REFERENCES

1. R. B. Tattersall, ed., "Fourth CSNI Specialist Meeting on Fuel-Coolant Interaction in Nuclear Reactor Safety," CSNI Report No. 37, for the OECD/NEA by the Atomic Energy Establishment Winfrith (1979).
2. J. E. Cahalan et al., "The Status and Experimental Basis of the SAS4A Accident Analysis Code System," Proceedings of the International Meeting on Fast Reactor Safety Technology, Seattle, Washington, August 19-23, 1979, pp. 603-614.
3. L. L. Smith, "The SIMMER-II Code and its Applications," Proceedings of the International Meeting on Fast Reactor Safety Technology, Seattle, Washington, August 19-23, 1979, pp. 187-196.
4. L. D. Buxton and V. B. Benedick, "Steam Explosion Efficiency Studies," Sandia National Laboratories, NUREG/CR-0947, SAND79-1399 (1979).
5. D. E. Mitchell, M. L. Corradini, and W. W. Tarbell, "Intermediate Scale Steam Explosion Phenomena: Experiments and Analysis," Sandia National Laboratories, NUREG/CR-2145, SAND81-0124 (1981).

6. R. G. Steinke, "Triangular Geometry Fluid Dynamics with Reduced Artificial Diffusion," Trans. Am. Nuc. Soc., 34, p. 311 (1980).
7. T. G. Theofanous, M. Saito, and T. Efthimiadis, "The Role of Hydrodynamic Fragmentation in Fuel Coolant Interactions," CSNI Report No. 37, for the OECD/NEA, by the Atomic Energy Establishment, Winfrith, pp. 112-128 (1979).
8. M. L. Corradini, "Analysis and Modeling of Steam Explosion Experiments," Sandia National Laboratories, NUREG/CR-2072, SAND80-2131 (1981).
9. T. P. Fishlock, "Calculations on Propagating Vapour Explosions for the Aluminum/Water and UO<sub>2</sub>/Sodium Systems," CSNI Report No. 37, for the OECD/NEA, by the Atomic Energy Establishment, Winfrith, pp. 54-79 (1979).
10. R. E. Henry and H. K. Fauske, "Core Melt Progression and the Attainment of a Permanently Coolable State," Proc. Topl. Mtg. Reactor Safety Aspects of Fuel Behavior, Sun Valley, Idaho, August 2-6, 1981, pp. 2-481 to 2-495.
11. F. S. Gunnerson and A. W. Cronenberg, "Film Boiling and Vapor Explosion Phenomena," Nuclear Technology, 49, pp. 380-391 (1980).
12. H. Jacobs, M. F. Young, and K. O. Reil, "Fuel-Coolant Interaction-Phenomena Under Prompt Burst Conditions" Proceedings of the International Meeting on Fast Reactor Safety Technology, Seattle, Washington, August 19-23, 1979, pp. 1520-1528.

### List of Figures

Fig. 1. Experimental thermite distribution from Ref. 5 compared with calculated results at explosion initiation for Mitchell Test MD-19.

Fig. 2. Water volume fractions in the Buxton simulation.

Fig. 3. Comparison of two experimental pressure traces from Ref. 4 with the calculated values from the present approach.

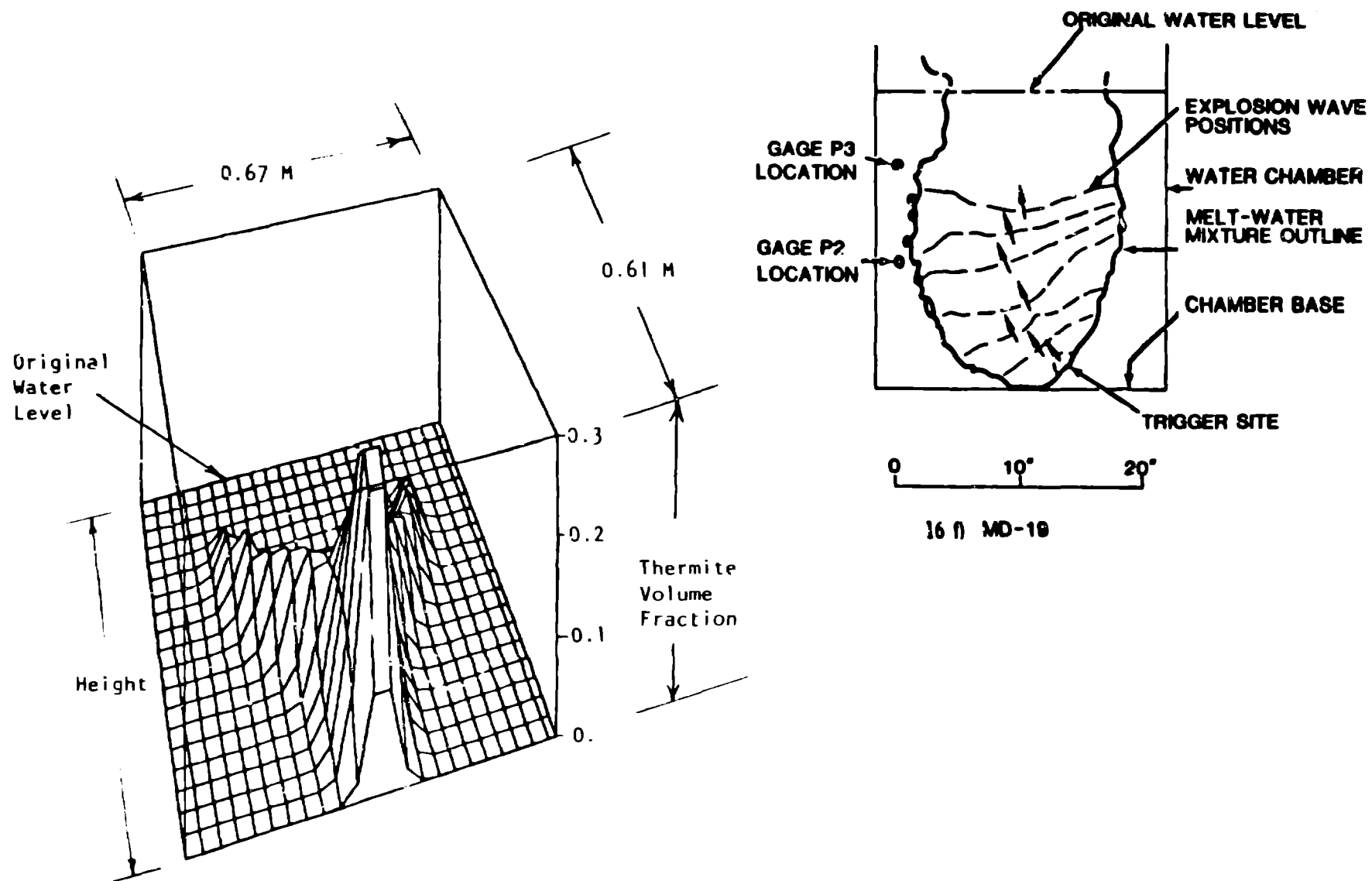


Fig. 1. Experimental thermite distribution from Ref. 5 compared with calculated results at explosion initiation for Mitchell Test MD-19.

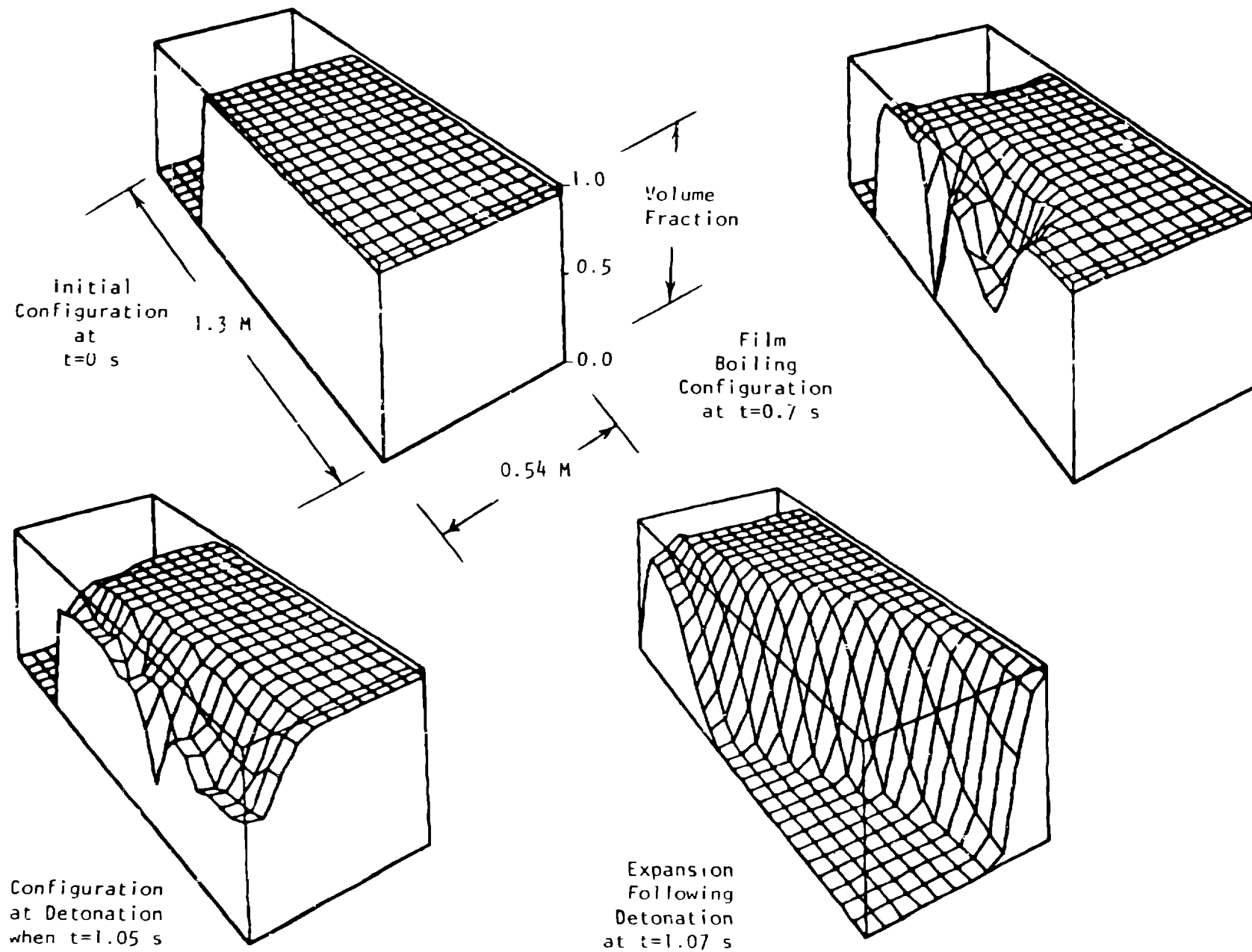


Fig. 2. Water volume fractions in the Buxton simulation.

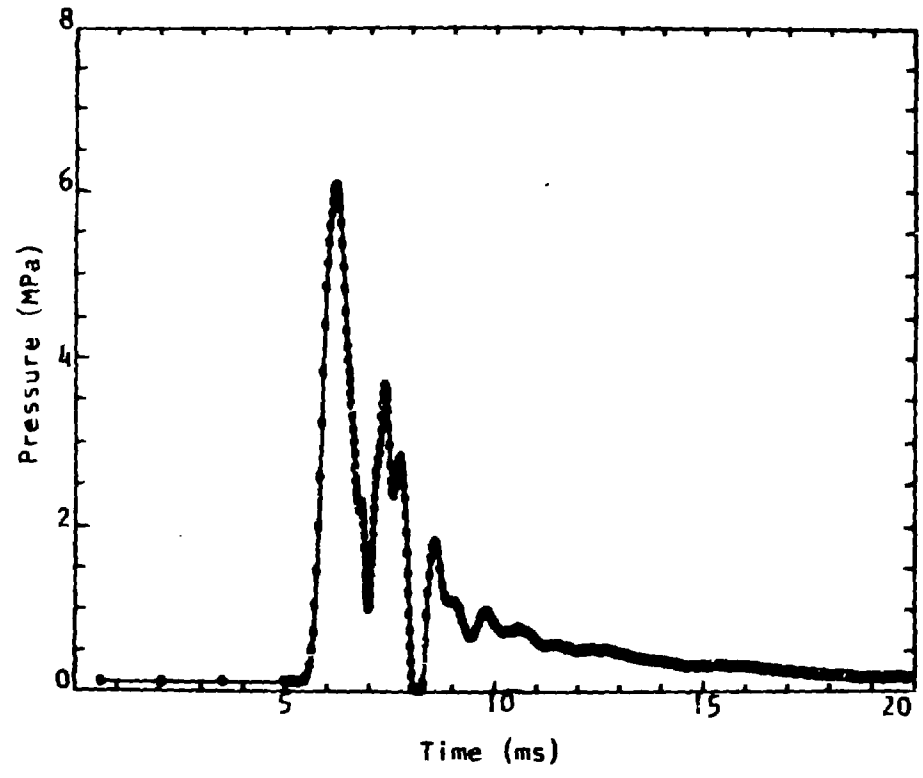
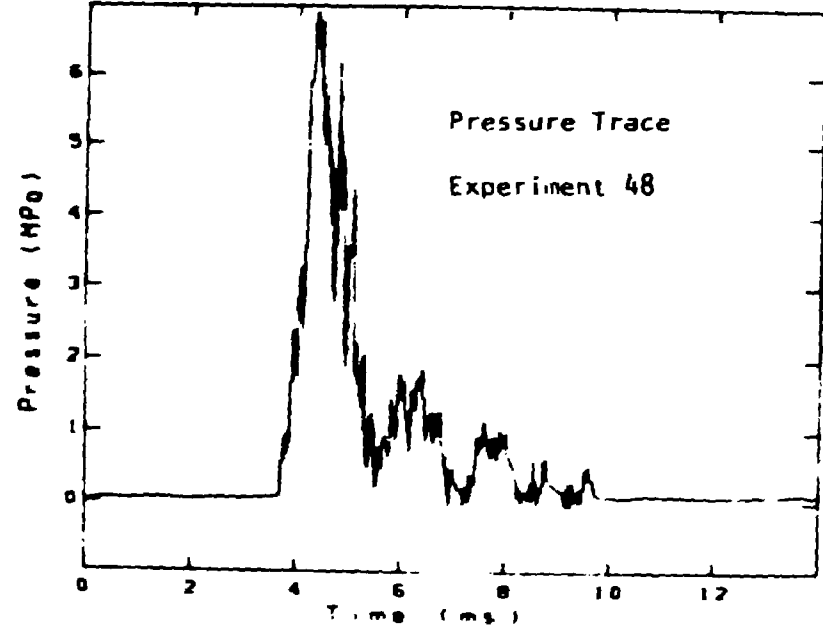
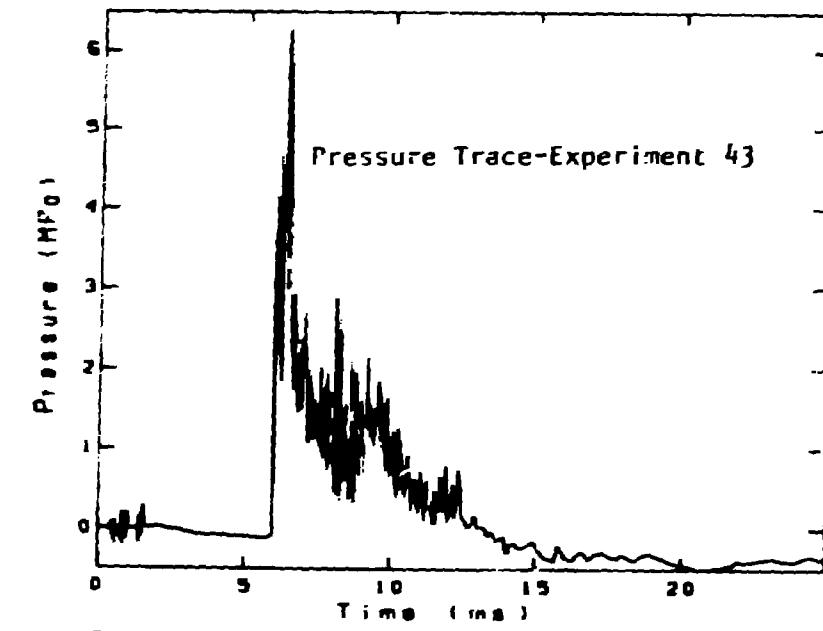


Fig. 3. Comparison of two experimental pressure traces from Ref. 4 with the calculated values from the present approach.